Broadband Guidance in a Hollow-Core Photonic Crystal Fiber With Polymer-Filled Cladding

Christos Markos, Grigorios Antonopoulos, and George Kakarantzas

***Abstract*— In this letter, we report for the first time (to the best of our knowledge) the ability of a conventional hollow-core photonic crystal fiber (HC-PCF) to guide light over a wide bandwidth by selectively filling the cladding of the fiber with polymeric material. The transmission spectrum of the new fiber was recorded using a supercontinuum source while the measured near-field profile, combined with the numerical analysis, verified the existence of a single white fundamental guided mode in the air-core. The main advantage of the proposed method is that broadband guidance in air can be easily achieved, avoiding complex and sophisticated designs as well as fabrication of the fiber cladding structure, thus opening new prospects for the HC-PCF.**

***Index Terms*— Optical fiber devices, optical polymers.**

I. Introduction

SOLID- and hollow-core photonic crystal fibers comprise a silica cladding with a periodic array of air-holes running down the entire length of the fiber [1]. Most of the research on combining PCFs with new materials has been focused on solid-core PCFs where infiltration of the cladding holes with functional materials such as liquid crystals [2], [3], metals [4], ferrofluids [5], polymers [6], [7], glasses [8], [9] etc. provides the possibility to manipulate and control the guiding properties of the PCF according to the required applications [10]. It has been also demonstrated by several groups that the air-channels of the HC-PCF can efficiently be used to host gas-phase materials for Raman or other non-linear applications [11], [15]. However, limited research has been carried out regarding hollow-core PCFs infused with advanced materials. Since 2002, it has been demonstrated that HC-PCF can guide light either by means of a photonic bandgap, or in the absence of a bandgap, via inhibited coupling guidance [12], [13]. In 2006, it was shown how the bandgap windows can be shifted (scaled down) to shorter wavelengths by infiltration of liquids with higher refractive index than air [16]. The former class of fibers though (bandgap guiding HC-PCF), exhibits a relatively narrow transmission window with low loss, while the latter (so called inhibited coupling HC-PCF or IC-HC-PCF) provide broadband guidance with higher transmission loss [17]–[19]. In contrast to bandgap fibers, the IC-HC-PCF cladding has no bandgap but instead exhibits low density of photonic states (DOPS) over a broad bandwidth along the air-line, indicating the little symmetry overlap between the core mode and the cladding modes in the respective frequency range [14], [15]. There are several reports on the fabrication of such IC-HC-PCFs that require a sophisticated and experienced handling in both the cladding structure design and in the fiber fabrication [18]–[22].

In this letter, we demonstrate that broadband guidance in air can be obtained simply by infiltrating the cladding of a commercially available bandgap HC-PCF with a polymer material of refractive index ~1.42. The polymer utilized in our experiments was poly-dimethylsiloxane (PDMS). The PDMS exhibits very good optical properties such as low absorption, high transparency with a refractive index lower than that of silica, low Young's modulus, etc. [23]–[25]. However, the most important feature of this material is its low shrinkage [25] which is an essential factor in our case. The loss of the polymer-filled HC-PCF is relatively higher than Kagome HC-PCF reported in the literature [15], [18], and [20]; however the main scope of this letter is to demonstrate the possibility of combining perhaps other functional materials such as polymers or glasses to further modify the guidance of the conventional HC-PCF with no need of the fabrication of a new fiber structure.

II. Experimental

In our experiments, we employed a 19-cell HC-PCF (similar 19-cell HC-PCF can be purchased from NKT photonics A/S) with core diameter d_C ~18 μm. The cladding holes have diameter of ~3.7 μm, strut width ~560 nm while the pitch of the fiber is ~4 μm. The cross section of the fiber is shown in Fig. 1.

In order to selectively fill the cladding region of the HC-PCF, we employed a UV curable polymer and a two-step infiltration-cure-cleave process as described in [26]. In the beginning, a UV-curing optical adhesive (NOA061) was infused at a length of a few mm's into the holes of the fiber by means of capillary forces. Due to the large diameter of the central hole, the optical adhesive travels faster, i.e. several millimeters more than in the cladding holes. At this point, we applied UV light from the side to cure the optical adhesive. Then we cleaved the fiber at the cleaving point as shown in Fig. 2(a). The cleaving point was determined by observing the filled length through the side of the fiber with an optical microscope. Since the core hole was blocked, we proceeded to infiltrate the PDMS material into the cladding holes.

Manuscript received March 8, 2013; revised August 9, 2013; accepted September 2, 2013. Date of publication September 5, 2013; date of current version September 25, 2013.

The authors are with the Theoretical and Physical Chemistry Institute, National Hellenic Research Foundation, Athens 116 35, Greece (e-mail: cmarkos@eie.gr; greganto@yahoo.com; gkakaran@eie.gr).

Color versions of one or more of the figures in this letter are available online at http://ieeexplore.ieee.org.

Digital Object Identifier 10.1109/LPT.2013.2280817

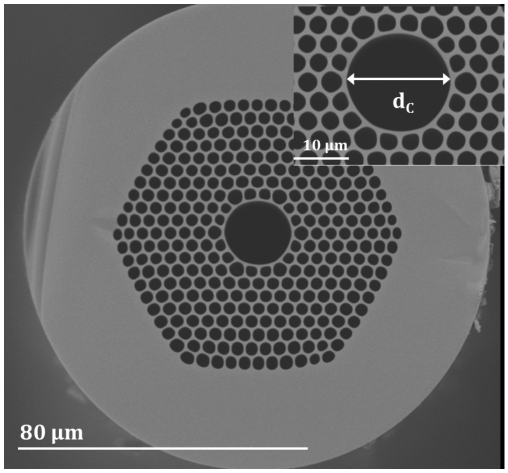

Fig. 1. Scanning electron microscopy (SEM) image of the HC-PCF. Inset: Magnified SEM image of the core.

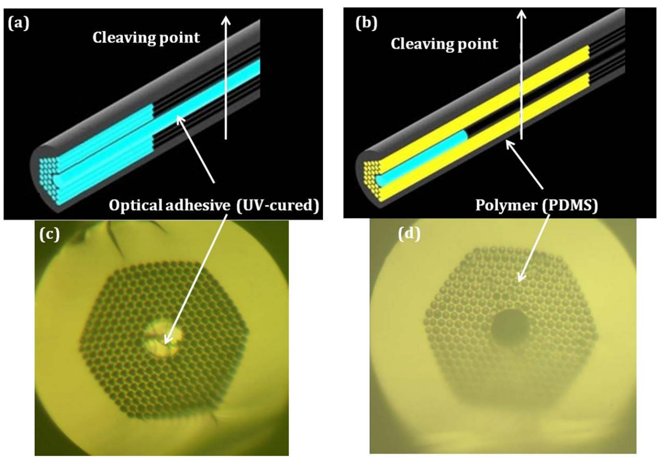

Fig. 2. Schematic representation of the selective filling process of (a) UV optical adhesive and (b) PDMS. The corresponding optical microscope images of the infiltrated (c) UV-optical adhesive core and (d) PDMS cladding.

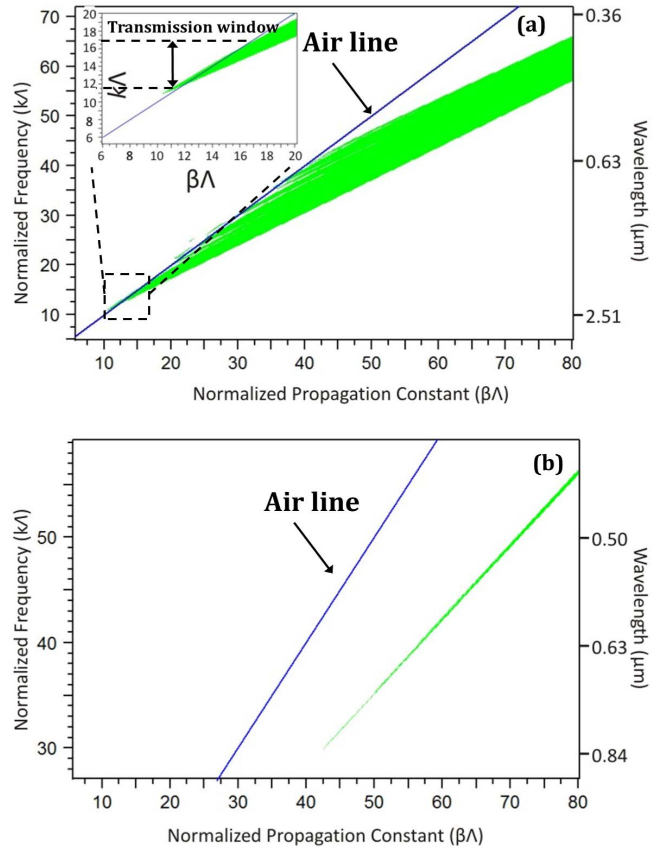

Fig. 3. (a) Calculated bandgaps (green color) for the conventional HC-PCF. Inset: Zoom-in of the crossing of the airline with the bandgap confirming the transmission window to be ~1400–1800 nm. (b) Calculated bandgaps in the case of PDMS-filled cladding unit cell. The solid line corresponds to the vacuum dispersion line in both cases.

The PDMS material was prepared by mixing 10:1 polymer with curing agent as described previously in [23]–[25]. Due to the high viscosity of the PDMS material, we inserted the fiber in a custom-made pressure cell, where the material infused into the holes at a pressure of ~14 bar. The PDMS infiltrated samples were left to cure for 48 hours at room temperature.

The second step involved another cleave as shown in Fig. 2(b). At the end of the process, the PDMS selectively filled only the cladding holes of the fiber. Fig. 2(c) and (d) correspond to the optical images of the fiber between the two cleaving points. The infused length of the HC-PCF with the polymer material was ~4 cm. In order to verify the polymer's uniformity and existence along the fiber, the latter was cleaved into several pieces along its length and observed at the optical microscope confirming the existence of the material inside the cladding of the fiber.

III. Numerical Determination of Bandgap Location

Prior to experimental work, we calculated the location of photonic bandgaps of the cladding unit cell using a plane-wave expansion method [27]. For each value of the propagation constant $\beta\Lambda$ (axial component of the wavenumber k normalized to the fiber pitch Λ), the band structure of the two-dimensional lattice of the HC-PCF was obtained by calculating the frequency eigenvalues of the vector Helmholtz equation. The band structure at each $\beta\Lambda$ was calculated by taking 16 points of the irreducible first Brillouin zone of the hexagonal fiber lattice, whereas $\beta\Lambda$ was scanned in steps of 0.2. Fig. 3(a) shows the "finger" plot (normalized propagation constant $\beta\Lambda$ vs. normalized frequency $k\Lambda$) of the HC-PCF before infiltrating the material in the cladding. Bandgaps are denoted in green color.

The transmission window of the fiber occurs in the infrared range 1400–1750 nm, which is where the vacuum dispersion line (or air-line) crosses the bandgap (see inset of Fig. 3(a)). Similarly, we repeated all the calculations, in the case where the cladding has been filled with PDMS. The refractive index of PDMS was taken to be ~1.42 [23]–[25] and that of fused silica 1.45. As it can been seen from Fig. 3(b), the bandgap region is now much shallower and away from the air-line. Since, in our case, the core of the fiber is made of air, no bandgap guidance can occur in the core.

IV. Broadband Guidance and Loss

We measured the transmission spectrum of this hybrid PDMS/silica structure using a supercontinuum source (SuperK compact, NKT Photonics A/S) covering the 500–1750 nm

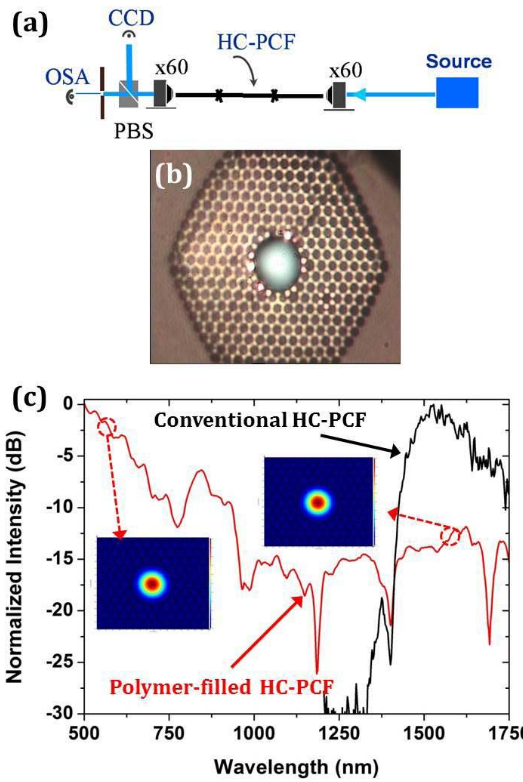

Fig. 4. (a) Experimental set-up. (b), near field pattern of the fundamental white light guided mode. (c) Transmission spectrum of the conventional (air/silica cladding) HC-PCF (black line) and the polymer-filled HC-PCF (red line). Insets: Calculated mode profiles of the polymer-filled HC-PCF at 600 and 1600 nm wavelength.

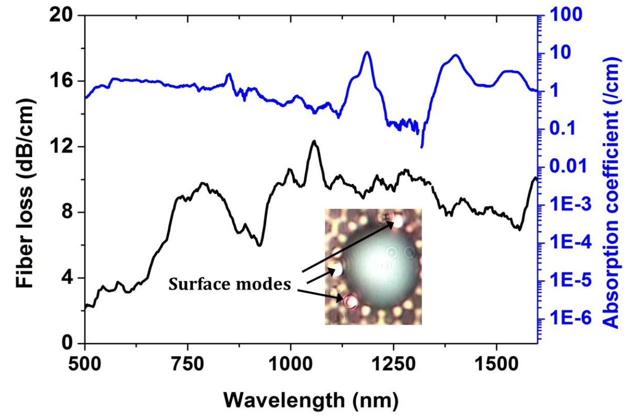

Fig. 5. (Color online) Loss profile of the PDMS-cladding filled HC-PCF (black line) and the absorption coefficient of the PDMS polymer material (blue line). Inset: Optical image of the strong surface modes in the silica strut.

wavelength range. The light was coupled in the fiber using an ×60 microscope objective. The output beam was collected with another ×60 microscope objective and a multimode fiber where the transmitted signal was recorded with an optical spectrum analyzer (OSA). All the undesired light (cladding and "surface" modes) was blocked by using an iris diaphragm into the beam path such that only light from the core was detected. In addition a beam splitter (BS) was inserted between the light output and OSA to record with a CCD camera the near field pattern. The experimental set-up is shown in Fig. 4(a). Fig. 4(b) shows the white-light near field intensity profile of the fundamental guided mode. It should be mentioned, that no higher order modes were observed by changing the launch conditions therefore the possibility of having dielectric capillary guidance can be excluded. Also, in capillary guidance the optical losses are at much higher levels compared to our case [29], [30].

Fig. 4(c) shows the acquired transmission spectrum of the polymer-filled HC-PCF. The insets of Fig. 4(c) show the calculated mode profiles of the polymer-filled HC-PCF at 600 and 1600 nm. The numerical mode calculation of the polymer-filled and conventional HC-PCF structure was done by employing the fully vectorial integrated mode solver of the commercially available Lumerical MODE solutions software. The effective indices of the fundamental guided modes are computed based on finite difference analysis using Yee's mesh and the index averaging technique [28]. The effective refractive index of the conventional HC-PCF at 1600 nm wavelength was found to be around 0.997317 while for the polymer-filled fiber was 0.9976460. Furthermore, as can be seen in Fig. 4(c), the spectrum exhibits transmission dips at around 1186, 1403, and 1690 nm. These observed dips may be the result of modal cutoffs of the different cladding resonators [14].

Inhibited coupling guidance in a HC-PCF, occurs when there is weak mode interaction between the core and the cladding over a certain frequency range. This type of guidance was first observed in the so-called Kagome fibers [15]. Contrary to the usual bandgap guiding HC-PCFs, which comprise a cladding with a hexagonal array of circular air holes in silica, the cladding of Kagome fibers consists of a square array of star-of-David silica strands in air. In this case, the strategy for weakening the coupling between the core modes and the cladding modes focuses on minimizing the size of the main glass resonators of the cladding structure. Inhibited coupling structures can exhibit much broader transmission windows than bandgap guiding HC-PCF [15], [22]. This is due to the fact that the cladding resonators associated with narrowing the bandgap range (for example, glass struts) are now much smaller [15]. We believe that the observed broadband guidance in our polymer-filled HC-PCF is possibly due to inhibited coupling between the fiber core and the cladding. It seems that there is now a different route for inhibiting the coupling of energy from the air guided mode to the cladding modes: Apparently, once the air is replaced with PDMS in the cladding, the number of available cladding modes near the air dispersion line is significantly reduced compared to the original air/silica structure. This in turn results in reduced coupling between the air-guided core modes and the modes supported by the PDMS/silica cladding over a broad wavelength range which is the actual transmission window of the polymer filled fiber.

We also measured the loss of the fiber using the cut-back technique. The minimum loss is ∼2.5 dB/cm at the visible range as shown in Fig. 5. We believe that these levels of loss may be introduced mostly due to confinement and absorption.

Another significant factor could be the intense surface modes that exist on the first ring of the silica strut. Additional loss maybe introduced by imperfections of the cleaved end facet of the hybrid HC-PCF due to the different mechanical properties of silica and PDMS. Further optimization in terms of loss is under progress by improving the infiltration and the material synthesis procedure.

V. Conclusion

In this letter, we presented for the first time to our knowledge broadband guidance in the air core of conventional HC-PCF with a PDMS polymer-filled cladding. The polymer inclusions introduce low index contrast in the cladding and consequently reduce significantly the DOPS. Therefore, the guidance mechanism is possibly relying on inhibiting coupling [14], [15]. We measured the transmission spectrum from 500–1750 nm and recorded the near-field profile confirming the existence of the broadband fundamental mode. In conclusion, the proposed new methodology provides a new highway for broadband guidance of light in air using conventional HC-PCFs selectively filled with advanced materials. The proposed technique could be useful in all applications that require guidance in air over an extended bandwidth.

References

[1] J. C. Knight, T. A. Birks, P. St. J. Russell, and D. M. Atkin, "All-silica single-mode optical fiber with photonic crystal cladding," *Opt. Lett.*, vol. 21, no. 19, pp. 1547–1549, 1996.

[2] W. Yuan, L. Wei, T. T. Alkeskjold, A. Bjarklev, and O. Bang, "Thermal tunability of photonic bandgaps in liquid crystal infiltrated microstructured polymer optical fibers," *Opt. Express*, vol. 17, no. 22, pp. 19356–19364, 2009.

[3] T. T. Larsen, A. Bjarklev, D. S. Hermann, and J. Broeng, "Optical devices based on liquid crystal photonic bandgap fibres," *Opt. Express*, vol. 11, no. 20, pp. 2589–2596, 2003.

[4] H. W. Lee, M. A. Schmidt, and P. St. J. Russell, "Excitation of a nanowire 'molecule' in gold-filled photonic crystal fiber," *Opt. Lett.*, vol. 37, no. 14, pp. 2946–2948, 2012.

[5] A. Candiani, M. Konstantaki, W. Margulis, and S. Pissadakis, "A spectrally tunable microstructured optical fibre Bragg grating utilizing an infiltrated ferrofluid," *Opt. Express*, vol. 18, no. 24, pp. 24654–24660, 2010.

[6] P. S. Westbrook, B. J. Eggleton, R. S. Windeler, A. Hale, T. A. Strasser, and G. L. Burdge, "Cladding-mode resonances in hybrid polymer-silica microstructured optical fiber gratings," *IEEE Photon. Technol. Lett.*, vol. 12, no. 5, pp. 495–497, May 2000.

[7] C. Markos, K. Vlachos, and G. Kakarantzas, "Guiding and birefringent properties of a hybrid PDMS/silica photonic crystal fiber," *Proc. SPIE*, vol. 7914, p. 791427, Feb. 2011.

[8] N. Granzow, P. Uebel, M. A. Schmidt, A. S. Tverjanovich, L. Wondraczek, and P. S. J. Russell, "Bandgap guidance in hybrid chalcogenide-silica photonic crystal fibers," *Opt. Lett.*, vol. 36, no. 13, pp. 2432–2434, 2011.

[9] I. Konidakis, G. Zito, and S. Pissadakis, "Photosensitive, all-glass $AgPO_3$/silica photonic bandgap fiber," *Opt. Lett.*, vol. 37, no. 13, pp. 2499–2501, 2012.

[10] B. T. Kuhlmey, B. J. Eggleton, and D. K. C. Wu, "Fluid-filled solid-core photonic bandgap fibers," *J. Lightw. Technol.*, vol. 27, no. 11, pp. 1617–1630, Jun. 1, 2009.

[11] F. Benabid, J. C. Knight, G. Antonopoulos, and P. St. J. Russell, "Stimulated Raman scattering in hydrogen-filled hollow-core photonic crystal fiber," *Science*, vol. 298, pp. 399–402, Oct. 2002.

[12] T. Grujic, B. T. Kuhlmey, A. Argyros, S. Coen, and C. M. de Sterke, "Solid-core fiber with ultra-wide bandwidth transmission window due to inhibited coupling," *Opt. Express*, vol. 18, no. 25, pp. 25556–25566, 2010.

[13] L. Vincetti and V. Setti, "Extra loss due to Fano resonances in inhibited coupling fibers based on a lattice of tubes," *Opt. Express*, vol. 20, no. 13, pp. 14350–14361, 2012.

[14] G. J. Pearce, G. S. Wiederhecker, C. G. Poulton, S. Burger, and P. St. J. Russell, "Models for guidance in kagome-structured hollow-core photonic crystal fibres," *Opt. Express*, vol. 15, no. 20, pp. 12680–12685, 2007.

[15] F. Benabid and P. J. Roberts, "Linear and nonlinear optical properties of hollow core photonic crystal fiber," *J. Modern Opt.*, vol. 58, no. 2, pp. 87–124, 2011.

[16] G. Antonopoulos, F. Benabid, T. A. Birks, D. M. Bird, J. C. Knight, and P. S. J. Russell, "Experimental demonstration of the frequency shift of bandgaps in photonic crystal fibers due to refractive index scaling," *Opt. Express*, vol. 14, no. 7, pp. 3000–3006, 2006.

[17] T. D. Hedley, D. M. Bird, F. Benabid, J. C. Knight, and P. St. J. Russell, "Modelling of a novel hollow-core photonic crystal fibre," in *Proc. CLEO/QELS*, Baltimore, MD, USA, 2003, pp. 1–3, paper QTuL4.

[18] F. Couny, F. Benabid, and P. S. Light, "Large-pitch kagome-structured hollow-core photonic crystal fiber," *Opt. Lett.*, vol. 31, no. 24, pp. 3574–3576, 2006.

[19] A. Argyros, S. G. Leon-Saval, and M. A. van Eijkelenborg, "Twin-hollow-core optical fibres," *Opt. Commun.*, vol. 282, no. 9, pp. 1785–1788, 2009.

[20] Y. Y. Wang, N. V. Wheeler, F. Couny, P. J. Roberts, and F. Benabid, "Low loss broadband transmission in hypocycloid-core Kagome hollow-core photonic crystal fiber," *Opt. Lett.*, vol. 36, no. 5, pp. 669–671, 2011.

[21] A. Argyros and J. Pla, "Hollow-core polymer fibres with a Kagome lattice: Potential for transmission in the infrared," *Opt. Express*, vol. 15, no. 12, pp. 7713–7719, 2007.

[22] A. Argyros, S. G. Leon-Saval, J. Pla, and A. Docherty, "Antiresonant reflection and inhibited coupling in hollow-core square lattice optical fibres," *Opt. Express*, vol. 16, no. 8, pp. 5642–5648, 2008.

[23] C. Markos, K. Vlachos, and G. Kakarantzas, "Guiding and thermal properties of a hybrid polymer-infused photonic crystal fiber," *Opt. Mater. Express*, vol. 2, no. 7, pp. 929–941, 2012.

[24] C. Markos, K. Vlachos, and G. Kakarantzas, "Bending loss and thermo-optic effect of a hybrid PDMS/silica photonic crystal fiber," *Opt. Express*, vol. 18, no. 23, pp. 24344–24351, 2010.

[25] F. Schneider, J. Draheim, R. Kamberger, and U. Wallrabe, "Process and material properties of polydimethylsiloxane (PDMS) for Optical MEMS," *Sens. Actuators A, Phys.*, vol. 151, no. 2, pp. 95–99, 2009.

[26] Y. Huang, Y. Xu, and A. Yariv, "Fabrication of functional microstructured optical fibers through a selective-filling technique," *Appl. Phys. Lett.*, vol. 85, no. 22, pp. 5182–5184, 2004.

[27] J. Broeng, S. E. Barkou, T. Sondergaard, and A. Bjarklev, "Analysis of air-guiding photonic band gap fibres," *Opt. Lett.*, vol. 25, no. 2, pp. 96–98, 2000.

[28] Z. Zhu and T. Brown, "Full-vectorial finite-difference analysis of microstructured optical fibers," *Opt. Express*, vol. 10, no. 17, pp. 853–864, 2002.

[29] E. A. Marcatilli and A. Schmeltzer, "Hollow metallic and dielectric waveguides for long distance optical transmission and lasers," *Bell Syst. Tech. J.*, vol. 43, pp. 1783–1809, Jul. 1964.

[30] A. Dutt, S. Mahapatra, and S. K. Varshney, "Capillary optical fibers: Design and applications for attaining a large effective mode area," *J. Opt. Soc. Amer. B*, vol. 28, no. 6, pp. 1431–1438, 2011.